Sensors and Actuators B 178 (2013) 547–554

Contents lists available at SciVerse ScienceDirect

Sensors and Actuators B: Chemical

journal homepage: www.elsevier.com/locate/snb

Electrodeless dielectrophoretic concentrator for analyte pre-concentration on poly-silicon nanowire field effect transistor

Srinivasu Valagerahally Puttaswamy[a], Chih-Heng Lin[b], Shilpa Sivashankar[a], Yuh-Shyong Yang[b,*], Cheng-Hsien Liu[a,*]

[a] Department of Power Mechanical Engineering, National Tsing Hua University, Hsinchu 300, Taiwan
[b] Laboratory of Enzyme, Proteomics and Bio-Electronics, National Chiao Tung University, Hsinchu 300, Taiwan

ARTICLE INFO

Article history:
Received 24 August 2012
Received in revised form 3 January 2013
Accepted 7 January 2013
Available online 16 January 2013

Keywords:
FET biosensors
iDEP
Sensitivity
Maskless photolithography

ABSTRACT

The sensitivity of biosensors can be affected by mass transport limitations as a result of miniaturization. To enhance signal sensitivity, pre-concentration of deoxyribonucleic acid (DNA), in the vicinity of the sensing elements of n-type polycrystalline silicon nanowire field effect transistor (Poly-Si NWFET) is demonstrated using a microfluidic device based on insulator or gradient dielectrophoresis (iDEP) to overcome mass transport limitations. In insulator-based dielectrophoresis (iDEP), insulating microstructures produce non-uniform electric fields to drive dielectrophoresis (DEP) in microsystems. Fabrication of accurately controlled three-dimensional (3D) microstructure of poly (ethylene glycol) diacrylate (PEG-DA) with a narrow microchannel using maskless gray-scale lithography is described. The fabrication of three-dimensional structures at low cost with saving time is accomplished by the use of maskless exposure system. PEG-DA has been used due to its excellent biocompatibility and ease of fabrication. To enhance the stability of PEG-DA, we added another polymer pentaerythritol tetraacrylate (PETA). Electrical property of the Poly-Si NWFET is ensured by plotting I–V_G curve after the integration of iDEP micro device.

1. Introduction

In recent years intensive efforts have been focused on the development of ultrasensitive biological sensors having wide variety of potential applications that range from genotyping to molecular diagnostics [1–3]. Development of field-effect transistors (FETs) built on Si nanowire (NW) channels has received lots of attention that improve current methods of DNA, viruses and proteins detection. The simplest assay that can be performed with FET biosensor is the direct (label-free) electrical detection of biomolecules using miniaturized bioelectronics devices modified with bioaffinitive agents that produce measurable electrical signals upon interacting with target biomolecules. However, these biosensors suffer from certain limitations such as device-to-device uniformity, the variations in the device fabrication processes, poor device uniformity, yield and scalability which hinder further development of these biosensors into practical systems [4]. The aspect of mass transport limitations on the sensitivity of biosensor with miniaturized sensor arrays has been reported previously [5–7]. Miniaturization of device improves signal transduction and sensitivity in many detection platforms, however due to improper concentration only few analyte molecules diffuse toward the miniaturized sensor surface for hybridization thereby slows down binding kinetics, delayed signal onset and saturation.

This infers that, in order to further enhance the sensitivity of biosensors, methods to concentrate target biomolecules toward the sensor surface are necessary. For protein sensors, improved transport becomes even more imperative for proteins, which diffuse at a rate which is an order of magnitude slower. A micromixing technique based on cavitation microstreaming principle [8] and high flow rate by using microfluidic channels made of polycarbonate [9] has been reported to accelerate hybridization process. However, no significant improvement has been observed. The electric field generated by the underlying microelectrodes to cause electrophoretic transport of molecules to the desired locations has been documented [10]. Moreover, the need of permanent layer and a non-conducting buffer limits its future applications. In the above approaches, different methods have been tried to enhance DNA hybridization kinetics whilst they have their limitations emphasizing the importance of enhancing the performance of biosensors.

DEP results in the movement of bio-particles under non-uniform electric fields and defined as “the motion of suspensoid particles relative to that of the solvent resulting from polarization forces

* Corresponding authors. Tel.: +886 3 5742496; fax: +886 3 5722840.
E-mail addresses: ysyang@faculty.nctu.edu.tw (Y.-S. Yang), liuch@pme.nthu.edu.tw (C.-H. Liu).

0925-4005/$ – see front matter © 2013 Elsevier B.V. All rights reserved.
http://dx.doi.org/10.1016/j.snb.2013.01.016

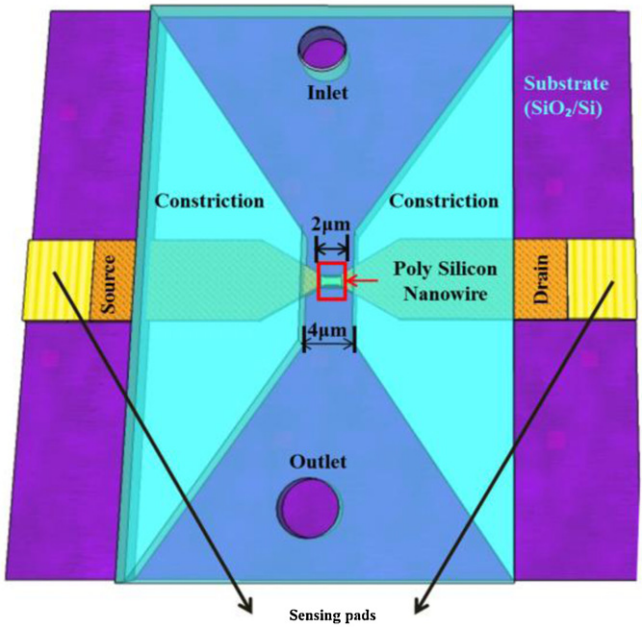

Fig. 1. Illustration of integration of iDEP microsystem with Poly-Si NWFET for pre-concentration of double stranded DNA.

produced by an inhomogeneous electric field" [11]. The DEP forces can be induced by both alternating current (AC) and direct current (DC) fields. It finds a wide range of applications [12] such as, separation and isolation of cells [13,14] cell handling prior to electro fusion and cell sorting [15]. DEP can be applied to a many group of materials as it utilizes intrinsic dielectric properties of the material. Applications of DEP in bioparticle sorting or manipulation using microdevices do not require stamping of the bioparticles, however stamping could often benefit in improved characterization of the DEP response of bioparticles. In addition, it is relatively uncomplicated to implement DEP in microdevices, wherein high-fields can be generated by metal electrodes separated by a few microns. The conventional method of metal electrodes-based DEP for force generation has been substituted recently by using insulating structures to generate localized DEP force fields, called electrodeless DEP (EDEP) or iDEP. The electrokinetic technique iDEP was, first proposed by Masuda et al. [16] and reviewed by Lee et al. employing spatially non-uniform insulating structures to produce non-uniform electric field by energized remote electrodes [17]. The devices are made of insulating materials, fabricated economically, promoting high-throughput and wide range of applications. The iDEP technique was employed to selectively trap and concentrate both live and dead *Escherichia coli* (*E. coli*) cells using microchannels containing arrays of circular insulating posts [18].The iDEP phenomenon for DNA molecules, *E. coli* cells, and blood cells using insulating structures and AC electric fields has been demonstrated by Chou et al. [19]. The microfluidic channels filled with insulating glass beads and AC electric fields were used for separating and concentrating yeast cells in water [20]. In another approach, on-chip iDEP with DC electric fields using arrays of insulating posts inside a microchannel to trap polystyrene particles was demonstrated experimentally and analytically [21]. The iDEP device with a converging sawtooth microchannel was used for separating mixtures of bio-particles and demonstrated using bacterial cells as a model system for separating biological structures [22]. There are many advantages of iDEP technique used to pre-concentrate biomolecules such as, prevention of metal evaporation during the fabrication process, application of high electric field without gas formation due to electrolysis at metal DEP electrodes, chemically inert and mechanically strong material. This technique is more appropriate for bio-particle pre-concentration because of simplistic fabrication and the absence of metallic objects which cause electrochemical reactions. This research work utilizes iDEP in which constriction made of PEG-DA is used as an insulating material instead of metal electrodes to restraint the electric field, thereby creating a maximum electric field at the narrow region. The insulating structure of PEG-DA is used to shape the electric field and to pre-concentrate DNA within a micro-constricted fluidic channel onto nanowire region of Poly-Si NWFET. The iDEP microdevice is integrated with Poly-Si NWFET which is fabricated without any expensive lithography tools employed to define nano-scale patterns. We have taken the advantage of insulating structure to shape the electric field, and allow the electrodes to be placed at a distance from the desired area of concentration [23–25]. The electrodes are placed at a distance from the sensing zone to minimize the impact of reactions and electrolytic bubble formation. Simulation results were used to influence the development of micro structure designs, so that miniaturization was optimized for the concentration of biomolecules, as well as for improved signal transduction.

2. Materials and methods

2.1. Concept

To verify the DEP effect induced by the electric-field gradients and for predicting the region of high field strength, a commercial finite element software CFD-ACE+ (CFDRC, Huntsville, AL) was used to simulate the induced electric field using the device prototype represented in Fig. 1. The CFD-ACE+ simulation software has wide range of application and has been used by our group to simulate electric field distribution and microfluidic flow pattern. While simulating for iDEP phenomena the following boundary conditions are set: (a) the boundary conditions on the channel walls are set to zero flow velocity based on a non-slipping assumptions. (b) The iDEP force is applied via AC potentials on the electrodes placed at the inlet and the outlet. (c) The boundary conditions at the inlet and outlet are set up as fixed pressure. CFD-ACE+ simulation result shows profiles along the microchannel, the focusing fields (electric field and field gradient) indicated by different colors. The electric field strength was maximum at the narrow region which is greatly essential for focusing bio-particles.

The layout consists of a single insulating structure in a unit cell of 400 μm × 600 μm × 40 μm (xyz). The insulating structure of PEG-DA is fabricated, aligned and integrated with Poly-Si NW FET. The gap of the constriction is gradually varied to study the resulting trends of field focusing factors due to the variation of these sizes. The electric potential was applied across the constriction at both ends of the unit cell. Fig. 2(a) represents the simulation result for a structure of 4 μm width constriction at the focusing region. The electric field was highly focused at the constriction as evident from the simulation result. It was apparent from Fig. 2(b) that a narrower insulator constriction is preferred since this would enhance the force fields. Though the field strength was maximum for 2 μm constriction we have used 4 μm constriction during the experiment to compensate for the misalignment. The vertical DEP field supporting, the efficacy of DNA pre-concentration through the microfluidics channel is represented in Fig. 2(c).

2.2. Materials

PEG-DA with a molecular weight of 575 was purchased from Sigma to be used as a precursor. 2-Hydroxy-4′-(2-hydroxyethoxy)-2-methyl-1-propiophenone (Sigma–Aldrich) was used as a photo initiator. Pentaerythritol tetraacrylate (PETA) (MW 352.34, Sigma),

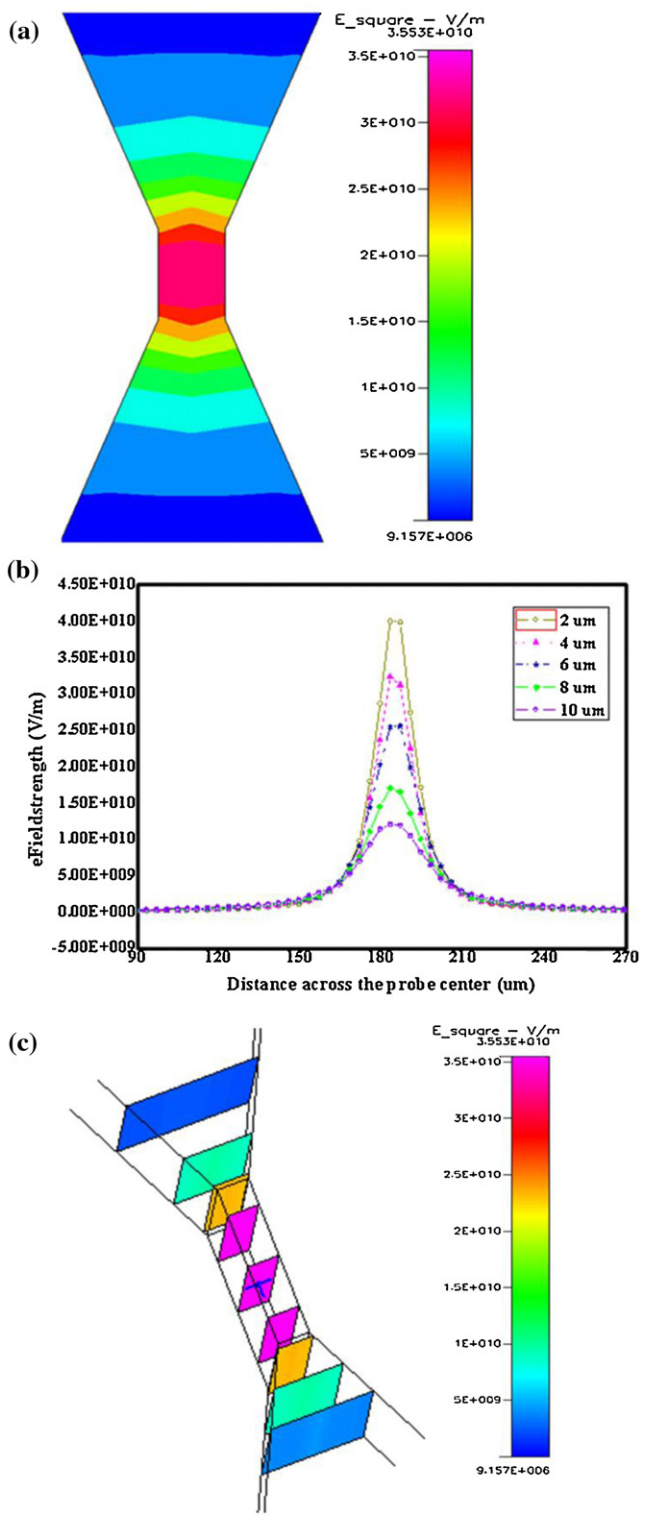

Fig. 2. (a) Electric field distribution around a single PEG-DA based iDEP trap. The narrow (focusing) region in the center of the channel with high electric field strength is for effectual concentration of analyte. (b) Electric field strength for varied distance of the constriction at the focusing region. The 4 μm channel is chosen for further experiments as it would be optimum for the poly Si-NWFET with 2 μm sensor width. (c) The vertical DEP field depicting the DNA pre-concentration for 4 μm constriction.

phosphate-buffered saline (PBS) (Applichem GmbH, Germany), sodium phosphate monobasic and sodium phosphate dibasic (J.T. Baker, USA) were also used during the experiment. All other solutions were prepared with DI water (resistance of water was 18.2 MΩ cm) from an ultra-pure water system (Barn-stead).

2.3. Fabrication of Poly-Si NWFET

The *n*-type Poly-Si NWFET was fabricated with complementary metal–oxide–semiconductor (CMOS)-compatible processes [26]. At first, the Si substrate was covered with a 100 nm silicon dioxide (SiO_2) layer and 80 nm silicon nitride (Si_3N_4) layer. Secondly, a SiO_2-dummy gate structure (length, 2 μm; width, 500 nm) was fabricated on the substrate. Further, an amorphous silicon (a-Si) layer (thickness, 100 nm) was deposited onto the substrate; the sample was then subjected to annealing at 600 °C to transmute the a-Si into poly-Si. The Poly-Si NWs and source/drain (S/D) contact areas were defined through a photolithography process and reactive plasma etching process. The two sidewall Poly-Si NW connected parallel were formed along the edges of the dummy gate structure using the sidewall spacer technique. The low-resistive Poly-Si areas used for S/D contacts were fabricated through ion implantation. Finally, the S/D contacts were passivated by a 150 nm SiO_2 layer to minimize both the leakage current [27] and noise in the solution environment. A schematic representation of the NW device prepared using the sidewall-spacer technique is illustrated in Fig. 3(a) and the SEM image of the NW device is elucidated in Fig. 3(b). The two parallel Poly-Si NWs are 2 μm in length. The vertical thickness and height of the Poly-Si NW were measured to be about 45 nm and about 70 nm, respectively as represented in Fig. 3(c), cross-sectional view of transmission electron microscopy (TEM) image.

2.4. Fabrication of iDEP insulating microstructure of PEG-DA

To generate PEG-DA microstructure, 1 ml of solution containing PEG-DA and PETA in PBS (pH 7.4) to yield final concentrations of 60%, 70%, 75%, 100% (w/w) was prepared prior to experiments in order to allow the PEG-DA to adequately dissolve in the solution. Immediately prior to UV photo polymerization, 10 μl of photo initiator solution was added to the PEG-DA solution (1 wt.%). Further the solution was introduced via inlet in between Poly-Si NWFET substrate and ITO glass separated by a spacer of 40 μm thickness. The ITO glass is used because of its reduced thickness which is convenient to drill inlet and outlet holes of 1 mm size. We have used SF-100 Xpress maskless photolithography system (Intelligent Micro Patterning, LLC, St. Petersburg) to fabricate iDEP constriction structure. The pattern data in bitmap was prepared on a personal computer using a general computer-aided design (CAD) software, followed by transferring the pattern data to the exposure system. This system incorporates smart filter technology comprising all of the necessary optical and electronic components needed to transfer an image onto the substrate by continuously generating the image frames by reflecting the UV laser light ($\lambda = 365$ nm) pixel by pixel. The projected image is free of distortion and uniform throughout the exposure area. A standard windows based personal computer is interfaced directly to the smart filter, providing system control and image storage for the exposure process. The alio stage works with the computer to take all the calculations and guesswork out of making multiple aligned exposures. If the area of image is less than the total desired exposure area, a step and repeat motion is used to expose substrate surfaces larger than the field of view. The auto stage software screens enable fully automated setup, calibration and execution of these activities. Changing the exposure patterns and the exposure time of each exposure makes the precise control of the profile of UV dose possible. Regions of PEG-DA exposed to UV underwent free-radical polymerization and became cross-linked, while unexposed regions were flushed out by deionized (DI) water and the desired PEG-DA based iDEP microstructure is constructed as illustrated in Fig. 4(a)–(d) and the fabrication steps were also illustrated with the schematic side view in Fig. 4(e). The variability of the PEG-DA constriction size after fabrication was estimated to be within ±1 μm. However, upon bonding

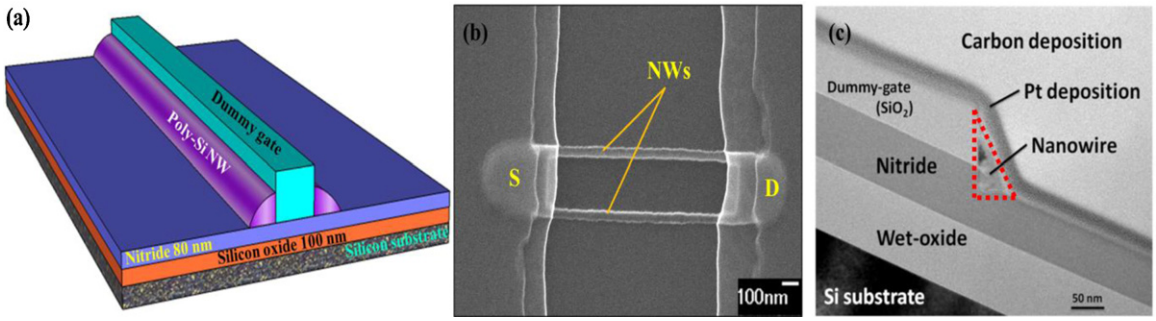

Fig. 3. Representation of the Poly-Si NWFET. (a) A schematic diagram illustrating different material components of *n*-type Poly-Si NWFET, fabricated using the sidewall-spacer technique, revealing two NWs fabricated in parallel along the dummy gate edges. (b) The SEM image of the Poly-Si NWFET representing two NWs connected to S and D electrodes. (c) TEM image to represent the vertical thickness and height of the Poly-Si NWFET.

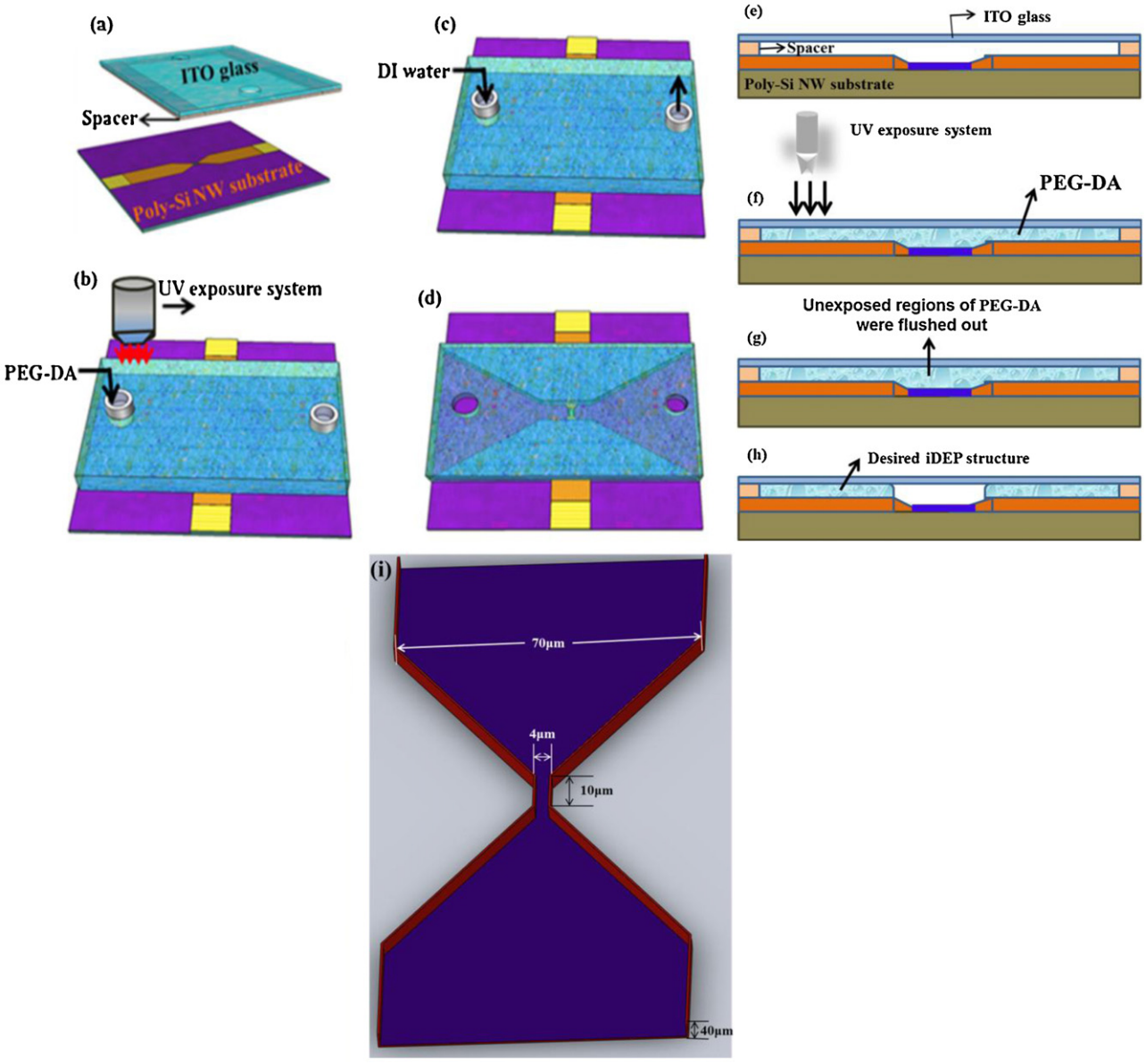

Fig. 4. Fabrication procedure of 3-dimentional iDEP microstructure using maskless photolithography. (a) The top glass drilled with inlet and outlet placed on the spacer. (b) PEG-DA introduced through the inlet to spread uniformly across the gap and continuous generation of frames by reflecting UV light pixel by pixel. (c) The exposed PEG-DA became cross-linked to solidify, whereas unexposed region was flushed out. (d) The precise iDEP structure was obtained. (e–h) Schematic diagram (cross sectional side view) of the fabrication steps. (i) Schematic representation for the cross-section of the microfluidics channel with important dimensions.

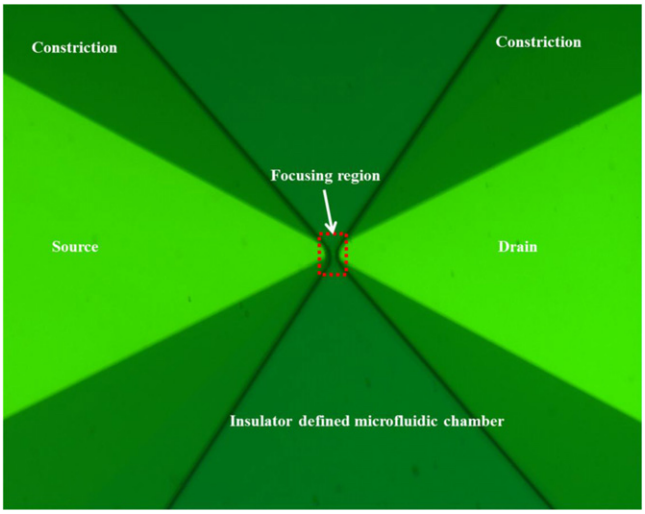

Fig. 5. Microscopic image depicting the integration of iDEP micro device with Poly-Si NWFET. The marked area represents the desired focusing region where poly-Si NW is situated.

to the substrate, an additional ±1 μm variation was observed in some cases. PEG-DA in native form is unbound to silicon surface calling in for the need of surface modification. Therefore, surface of silicon substrate had to be modified to achieve adhesion of PEG-DA microstructures on the substrate. In the first step, the substrate was treated with 2% 3-(trimethoxysilyl) propyl-methacrylate (TSM) (Sigma–Aldrich) for 2 min and in the second step, it was rinsed immediately with 99.9% ethanol and baked at 100 °C for 10 min. This process generates free methacrylate groups on the silicon substrate, which will react with PEG-DA during UV exposure and will prevent detachment of the hydrogel structures. The PEG-DA based iDEP structure was fabricated and aligned precisely with the Poly-Si NW as shown in Fig. 5. The use of SF-100 Xpress maskless photolithography system provides the user with the ability to perform photolithography processing without the need for expensive photomasks. This method enables fabrication of variable three-dimensional patterns at low cost with saving time which is especially advantageous for developing micro-electro-mechanical systems. The specific advantages of maskless photolithography over conventional photolithography with photomasks are tabulated in Table 1.

2.5. Working principle

Sample was introduced via the inlet reservoir. After sample introduction, pair of platinum wire electrodes were placed in each of the reservoir in contact with the solution and attached to a power supply. To observe DNA preconcentration at the constriction region, fluorescence measurements were performed using dye SYBR® Green I nucleic acid gel stain (Sigma–Aldrich), with double stranded DNA (20 bp) (MDBio, Inc.) in sodium phosphate buffer of 10 mM concentration (pH 7). The conductivity of the buffer is measured to be 1350 μS/cm using a conductivity meter Cond 330i (WTW GmbH, Germany, 0.5% accuracy) at room temperature. The AC voltage was set at the specified potential between 20–60 Vpp (peak to peak) at 100 Hz–2 MHz frequencies and was applied to the platinum electrodes. An inverted florescent microscope (BX-51, Olympus, Tokyo, Japan) was used to keep track of the motions and displacements of biomolecules. Images were captured and recorded via a digital CCD camera (Diagnostic Instruments Inc., USA) connected to a computer.

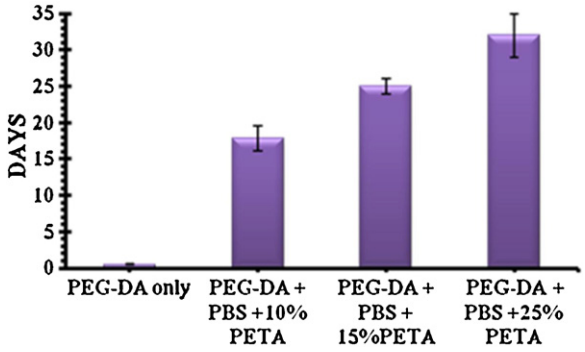

Fig. 6. Stability of PEG-DA based microstructures array in DI water at room temperature. The average and standard deviation were obtained from three samples for each condition. All data represent mean ± S.D ($n = 3$).

3. Results and discussion

3.1. Stability retention of PEG-DA microstructure

The fabricated PEG-DA microstructures were tested for stability in DI water at room temperature. The microstructures were immersed in DI water for 24 h and then by visual and microscopic observation the stability was assessed. After about 12 h, the microstructures fabricated by PEG-DA alone were observed to be unstable, delaminated, calling for certain modifications in order to enhance their stability. Therefore we added another polymer PETA with varying concentration to optimize the stability. Four types of PEG-DA precursors were prepared: (a) PEG-DA only, (b) PEG-DA + PBS + 10% PETA, (c) PEG-DA + PBS + 15% PETA, (d) PEG-DA + PBS + 25% PETA. The stability of the structures prepared with above composition was assessed by immersing them in DI water for stipulated number of hours. The average and standard deviations were obtained from three samples for each condition and the results are plotted as depicted in Fig. 6.

The microstructures were stable for a maximum period of 32 days in precursor type (d). In addition, to improve adhesion of the polymerized structures, the glass surface was pre-treated to acrylate it with TSM. The stability of the structure is increased to make the structure rigid against the flow of the medium. The four

Table 1
Comparison of maskless photolithography with the conventional photolithography.

Maskless photolithography	Conventional photolithography
No photomask is required and is more economical	Need of photomask resulting in increased cost and time involved in fabrication of mask.
Few minutes required for fabricating complicated microstructures	Takes few hours to fabricate microstructures
No contamination problem	Chances of contamination by mask
Mask disposal prevented	Disposal of mask is an additional problem
User may verify and control image to substrate alignment by using beam splitter and a camera	Precise alignment of mask is not possible due to manual movement
The scale of the image can be changed, useful for slight adjustment to small variations of substrate	The size of the mask is fixed and cannot be adjusted
Provided with fully automated controls	All the controls will have to be manually adjusted

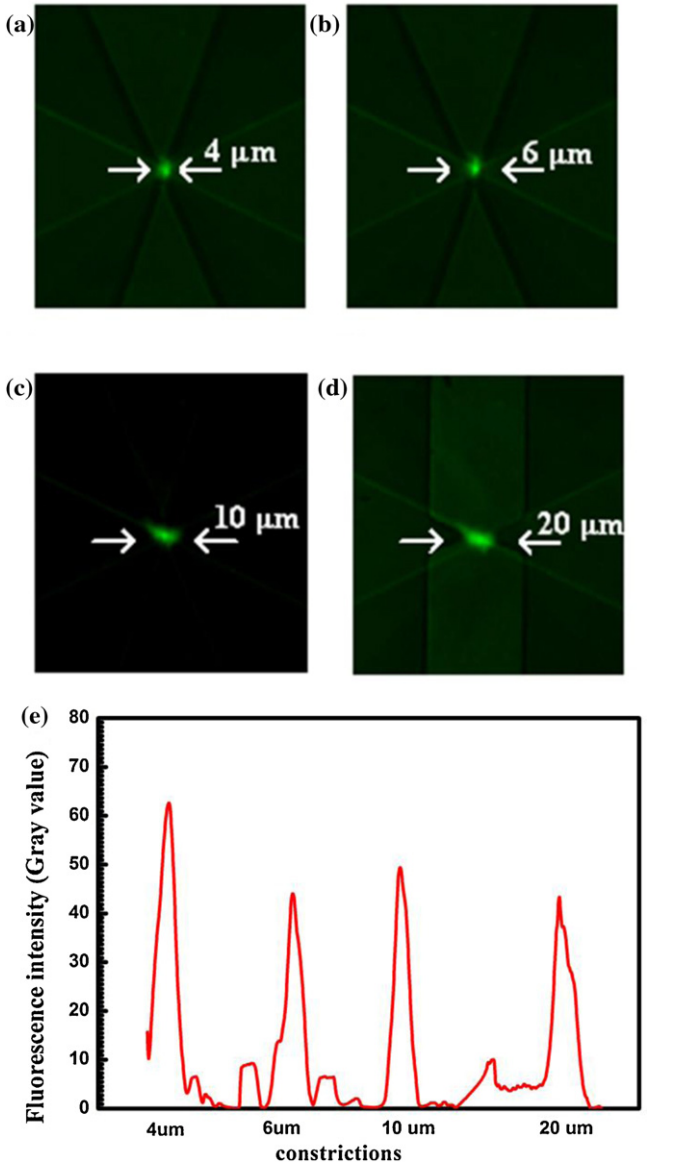

Fig. 7. Fluorescent images of pre-concentrated double-stranded DNA at various PEG-DA constricted microfluidic channels. (a)–(d) are the images of DNA focused at 4, 6, 10 and 20 μm, constriction respectively. (e) fluorescence signals intensity measured using Image-J software at all the constrictions.

acrylate terminals of PETA, a crisscross molecule, cross-links with PEG-DA resulting in denser mesh structure with tighter configuration. Due to this, the fabricated microstrucures demonstrated significant improvement of physical stability with 60% PEG-DA, 15% PBS and 25% PETA composition, without compromising its non-biofouling property. The time taken to fabricate these structures is very less (tens of min) unlike the conventional photolithography process (hours together). The mechanical strength and flexibility of the microstructures were controlled by its composition.

3.2. PEG-DA based iDEP pre-concentration of fluorescently labeled double-stranded DNA

The pre-concentration of fluorescently labeled double-stranded DNA was demonstrated. Good degree of DNA pre-concentration in relatively short times (1 min) was obtained in the buffer for the DEP conditions of 50 Vpp, 1 MHz. The pre-concentration of double-stranded DNA for different constriction size was analyzed

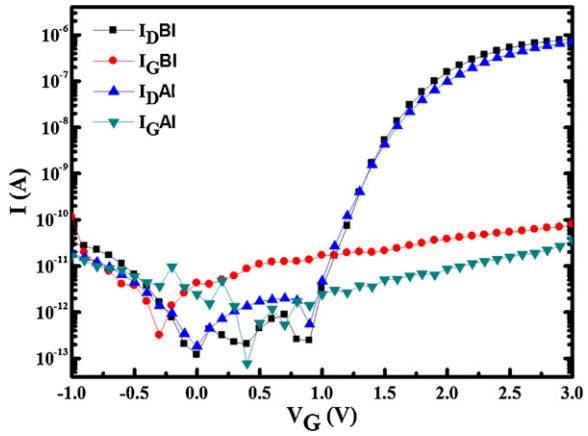

Fig. 8. I–V_G curve depicting excellent electrical characteristics and n-type behavior before integration (Bl) and after integration (Al) of iDEP microdevice.

in Fig. 7(a)–(e). The results in Fig. 7(a)–(d) vindicate significant pre-concentration within 5 min for the four constriction sizes of 4, 6, 10 and 20 μm for iDEP field conditions of 30 Vpp at 500 Hz.

To quantify the degree of pre-concentration, the fluorescence intensity of iDEP-concentrated DNA molecules (after back-ground intensity subtraction due to buffer, substrate, and electronic noise) was measured and compared using Image-J software, at all the iDEP constrictions and the quantitative data is represented in Fig. 7(e). With application of iDEP field conditions it was observed that the fluorescence intensity quantifying degree of DNA pre-concentration increased by 4 fold, 5 fold and 4 fold for constrictions of 6, 10 and 20 μm respectively. However for the constrictions of 4 μm, there was nearly 7 fold increase in DNA pre-concentration with application of iDEP field conditions as represented in Fig. 7(e).

From the figure it was clear that the fluorescence signals were peaked at the 4 μm constriction and showed the highest fluorescence intensity over all the other cases. This suggests a fact that the narrower iDEP structure is preferred as this would enhance the force field. We have taken the advantage of positive DEP effect for pre-concentration of DNA in a short span of time for which higher electric field strength at the narrow region is desired. A field of 50 Vpp, 1 MHz was required for a comparable degree of pre-concentration within a minute. However, high voltage of this order and higher pre-concentration times may effect complimentary DNA probes on the Poly-Si NW at the constriction possibly

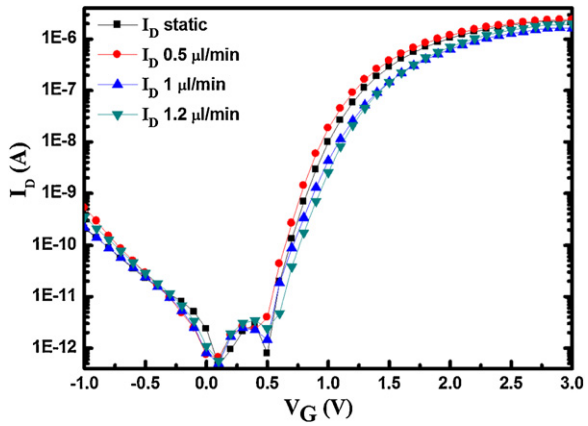

Fig. 9. I_D–V_G characteristics of Poly-Si NWFET at different flow rates. Sodium phosphate buffer introduced through the micro channel under a static and different flow rates after the integration of iDEP constriction structure. The device performance was maintained even under different flow conditions emphasizing the compatibility of the device for biosensing applications.

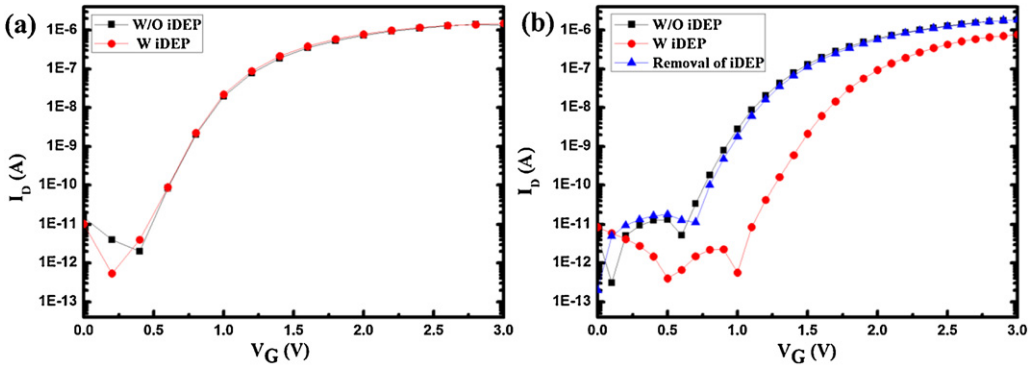

Fig. 10. Performance Comparison of Poly-Si NWFET device with and without the application of iDEP field conditions. (a) I_D–V_G characteristics of the control group with and without the application of iDEP. (b) I_D–V_G characteristics of the experimental group with and without the application of iDEP. The magnitude of lateral shift of I_D with the application of iDEP and subsequent pre-concentration of DNA on the NW is significant which substantiates the improved sensitivity of the Poly-Si NWFET.

due to electrolysis. Hence, field conditions of 30 Vpp at 500 Hz, is appropriate where a reasonable level of pre-concentration could be obtained within 5 min. It was observed that pre-concentration is stronger for 4 μm sized constriction compared with the others.

With the use of iDEP technique we achieved pre-concentration at desired sensing region rather than at the electrodes to prevent hazardous effect on the biosample and also on the performance of Poly-Si NWFET. From the experimental results, it was proved that the target DNA pre-concentration through constriction-based DEP was not handicapped by nanoscaled Poly-Si NW. Meanwhile, receded nanowire size for the purposes of improved sensitivity was not disadvantageous to iDEP as long as the nanowire was integrated to a mitigated insulator constriction in a microfluidic channel to amplify the focusing effects. As a consequence, the pre-concentration of low dielectric strength biomolecules (such as DNA), was undeterred by the lower biomolecular polarizability. The proposed iDEP technique for DNA pre-concentration was not hampered by joule heating and convective flow developed by the temperature gradients. All the above mentioned facts prove that the proposed method of constriction based iDEP is promising method for analyte pre-concentration and can be efficiently applied for wide class of biosensing pulpits. The future work is to assess the performance enhancement of Poly-Si NWFET integrated with iDEP microdevice during DNA hybridization. The electrical properties of Poly-Si NWFET in air, before and after integration was compared by plotting I–V_G curve with constant V_D = 0.5 V as elucidated in Fig. 8. From the result it was apparent that the device had shown excellent electrical characteristics with reduced leakage current.

Furthermore, In order to assess the performance of Poly-Si NWFET with a flow, after fabrication and integration of PEG-DA insulating structure, we have introduced sodium phosphate buffer of 10 mM concentration (pH 7) into the micro channel with a flow rates of 0.5 μl/min, 1 μl/min and 1.2 μl/min. The different flow rates are selected based on the optimized flowrates obtained during flowrate analysis on the proposed iDEP microdevice. I_D–V_G curve is plotted to valuate the performance of the device under different flow conditions. When the PEG-DA based constricted microchannel (4 μm width and 40 μm height) is used, as shown in Fig. 9 the device performance was perpetuated even under different flow conditions. From the experimental results we can conclude that, the performance of Poly-Si NWFET was not hindered by the fabrication and integration of iDEP microdevice and it can be efficiently used for biosensing application.

To test the efficacy of the iDEP microsystem with Poly-Si NWFET, I_D–V_G curve was plotted to assess the change in performance of the Poly-Si NWFET device with and without iDEP phenomenon. For the control group, sodium phosphate buffer of 10 mM concentration was introduced into the microchannel via inlet and the I_D–V_G curve is plotted with a constant bias voltage (V_D = 0.5 V) while sweeping gate potential (V_G) from 0 to 3 V, without the application of iDEP. In the next step, the iDEP field conditions of 30 Vpp at 500 Hz were applied, via pair of platinum wire electrodes placed in each of the reservoirs in contact with the buffer. The I_D–V_G curve is plotted and the result is represented in Fig. 10(a). For the experimental group, the double stranded DNA (20 bp) of 1 nM concentration in sodium phosphate buffer of 10 mM concentration (pH 7) was introduced via the inlet reservoir. The I_D–V_G curve is plotted with a constant bias voltage (V_D = 0.5 V) while sweeping gate potential (V_G) from 0 to 3 V, without the application of iDEP. Further, the iDEP field conditions of 30 Vpp at 500 Hz were applied for 5 min. The I_D–V_G curve is plotted and it was observed that the curve shifted laterally with a significant magnitude due to accumulation of DNA on the nanowire surface with the application of iDEP. Furthermore, when the iDEP field conditions were removed the I_D–V_G curve shift back to the base line as represented in Fig. 10(b). Compared to the control group, the I_D–V_G curve shifted significantly due to the pre-concentration of DNA, with the application of iDEP field conditions and reverted back to the base line on removal of iDEP field conditions, which substantiate the improved sensitivity of the Poly-Si NWFET. From the above result it is evident that the proposed method is very much useful for FET detection.

4. Conclusions

In summary, constriction-based iDEP device was integrated with Poly-Si NWFET to overcome mass transport limitations due to miniaturization, by significant pre-concentration of DNA to enhance its hybridization kinetics. Due to the high focusing fields obtained, the pre-concentration of low polarizability biomolecules such as DNA was demonstrated. The fabrication process was simple without resorting to advanced and costly lithography tools. The proposed method can be conveniently used for pre-concentration of bio-molecules which in turn enhance the sensitivity of Poly-Si NWFET.

Acknowledgements

The authors would like to thank the National Science Council of Taiwan (Grant No.98-2120-M-007-003) for its financial support. The authors thank Semiconductor Research Center and National Nano Device Laboratory for the access of microfabrication facility.

References

[1] J. Lu, G. Getz, E.A. Miska, E. Alvarez-Saavedra, J. Lamb, D. Peck, A. Sweet-Cordero, B.L. Ebert, R.H. Mak, A.A. Ferrando, J.R. Downing, T. Jacks, H.R. Horvitz,

T.R. Golub, MicroRNA expression profiles classify human cancers, Nature 435 (2005) 834–838.
[2] G. Hutvagner, P.D. Zamore, A cellular function for the RNA-interference enzyme Dicer in the maturation of the let-7 small temporal RNA, Science 293 (2001) 834–838.
[3] Y. Lee, C. Ahn, J. Han, Choi, H. Kim, J. Yim, J. Lee, P. Provost, O. Radmark, S. Kim, The nuclear RNase III Drosha initiates microRNA processing, Nature 425 (2003) 415–419.
[4] Z. Gao, A. Agarwal, A.D. Trigg, N. Singh, C. Fang, C.H. Tung, Y. Fan, K.D. Buddharaju, J. Kong, Silicon nanowire arrays for label-free detection of DNA, Analytical Chemistry 79 (2007) 3291–3297.
[5] J. Bishop, A. Chagovetz, S. Blair, Effects of fill fraction on the capture efficiency of nanoscale molecular transducers, Nanotechnology 17 (2006) 2442–2448.
[6] P.R. Nair, M.A. Alam, Effects of fill fraction on the capture efficiency of nanoscale molecular transducers, Applied Physics Letters 88 (2006) 233120.
[7] P.E. Sheehan, L.J. Whitman, Detection limits for nanoscale biosensors, Nano Letters 5 (2005) 803–807.
[8] R.H. Liu, R. Lenigk, R.L. Druyor-Sanchez, J.N. Yang, P. Grodzinski, Hybridization enhancement using cavitation microstreaming, Analytical Chemistry 75 (2003) 1911–1917.
[9] R. Lenigk, R.H. Liu, M. Athavale, Z.J. Chen, D. Ganser, J.N. Yang, C. Rauch, Y.J. Liu, B. Chan, H.N. Yu, M. Ray, R. Marrero, P. Grodzinski, Plastic biochannel hybridization devices: a new concept for microfluidic DNA arrays, Analytical Biochemistry 311 (2002) 40–49.
[10] M.J. Heller, A.H. Forster, E. Tu, Active microelectronic chip devices which utilize controlled electrophoretic fields for multiplex DNA hybridization and other genomic applications, Electrophoresis 21 (2000) 157–164.
[11] H.A. Pohl, The motion of precipitation of suspensoids in divergent electric fields, Journal of Applied Physics 22 (1951) 869–871.
[12] M.P. Hughes, Nanoelectromechanics in Engineering and Biology, CRC Press, United Kingdom, 2002.
[13] X.B. Wang, Y. Huang, J.P.H. Burt, Selective dielectrophoretic confinement of bioparticles in potential energy wells, Journal of Applied Physics 26 (1993) 1278–1285.
[14] G.H. Markx, Y. Huang, X.F. Zhou, Dielectrophoretic characterization and separation of micro-organisms, Microbiology 140 (1994) 585–591.
[15] M. Washizu, T. Nanba, S. Masuda, Handling biological cells using a fluid integrated circuit, IEEE Transformations on Industrial Applications 26 (1990) 352–356.
[16] S. Masuda, M. Washizu, T. Nanba, Novel method of cell fusion in field constriction area in fluid integrated circuit, IEEE Transformations on Industrial Applications 25 (1989) 732–737.
[17] S.W. Lee, S.D. Yang, Y.W. Kim, Y.K. Kim, Micromachined cell handling devices, in: Proc. 16th Annual International Conf. IEEE 2, Engineering in Medicine and Biology Society (1994), 1019–1020.
[18] E.B. Cummings, A.K. Singh, Dielectrophoresis in microchips containing arrays of insulating posts: theoretical and experimental results, Analytical Chemistry 75 (2003) 4724–4731.
[19] C.F. Chou, J.O. Tegenfeldt, O. Bakajin, S.S. Chan, E.C. Cox, N. Darnton, T. Duke, R.H. Austin, Electrodeless dielectrophoresis of single and double-stranded DNA, Biophysical Journal 83 (2002) 2170–2179.
[20] J. Suehiro, R. Hamada, D. Noutomi, M. Shutou, M. Hara, A selective detection of viable bacteria using dielectrophoretic impedance measurement method, Journal of Electrostatics 57 (2003) 157–168.
[21] E.B. Cummings, A.K. Singh, Dielectrophoretic trapping without embedded electrodes, in: Conference on Microfluidic Devices and Systems III. Proc. SPIE, Santa Clara, 2000, pp. 164–173.
[22] M.D. Pysher, M.A. Hayes, Electrophoretic and dielectrophoretic field gradient technique for separating bioparticles, Analytical Chemistry 79 (2007) 4552–4557.
[23] R.C. Gallo-Villanueva, C.E. Rodri' guez-Lopez, R.I. Dıaz-de-la-Garza, C. Reyes-Betanzo, B.H. Lapizco-Encinas, DNA manipulation by means of insulator-based dielectrophoresis employing direct current electric fields, Electrophoresis 30 (2009) 4195–4205.
[24] N. Calander, Analyte concentration at the tip of a nanopipette, Analytical Chemistry 81 (2009) 8347–8353.
[25] R.W. Clarke, J.D. Piper, L. Ying, D. Klenerman, Surface conductivity of biological macromolecules measured by nanopipette dielectrophoresis, Physical Review Letters 98 (2007) 198101–198104.
[26] C.Y. Hsiao, C.H. Lin, C.H. Hung, C.J. Su, Y.R. Lo, C.C. Lee, H.C. Lin, T.Y. Huang, Y.S. Yang, Novel poly-silicon nanowire field effect transistor for biosensing application, Biosensors and Bioelectronics 24 (2009) 1223.
[27] M.P. Lu, C.Y. Hsiao, P.Y. Lo, J.H. Wei, Y.S. Yang, M.J. Chen, Semiconducting single-walled carbon nanotubes exposed to distilled water and aqueous solution: electrical measurement and theoretical calculation, Applied Physics Letters 88 (2006) 053114.

Biographies

Srinivasu Valagerahally Puttaswamy received M.E. degree in mechanical engineering from Bangalore University, Bangalore India, in 2002. He is having experience as an assistant professor in an engineering college for six years. He is currently a Ph.D. candidate in the Power Mechanical Engineering from National Tsing-Hua University, Taiwan. His research interests are in liver lab chip, biosensors, tissue engineering, Bio-MEMS, microfluidics design and optoelectronic tweezers for biomedical applications.

Chih-Heng Lin received his master degree in Molecular Medicine and Bioengineering from National Chiao Tung University, Taiwan in 2006 and Ph.D. degree in Department of Biological Science and Technology at National Chiao Tung University in 2012, respectively. Presently he is a post-doctoral researcher in the Department of Biological Science and Technology at National Chiao Tung University. His research interests are in the area of biochemistry, molecular biology, and bioelectronics.

Shilpa Sivashankar received a B.E. degree in biotechnology from Sapthagiri College of Engineering, Bangalore, India in 2008 and M.S. degree in power mechanical engineering from National Tsing-Hua University, Taiwan. She is currently a Ph.D. candidate in the Department of Power Mechanical Engineering from National Tsing-Hua University, Taiwan. Her research interests include microfluidics, BioMEMS application for medical devices, tissue engineering, and biosensors.

Yuh-Shyong Yang received his master degree in Wood Science & Technology from University of California, Berkeley in 1983 and Ph.D. degree in Biochemistry from University of Wisconsin, Madison in 1987, respectively. Presently he is a professor in the Department of Biological Science and Technology at National Chiao Tung University. His research interest covers a wide variety of areas in Biological function of enzymes, proteomics, biodiversity, biosensing and bioelectronics. He is the recipient of Protein Science Young Investigator Travel Grant and Finn Wold Travel Award of 24th Protein Society Annual Symposium of the year 2010, Fellowship of Young Scientists Program 2009 in 21st IUBMB and the 12th FAOBMB International Congress of Biochemistry and Molecular Biology. One of his research article is selected as the featured Article in Nanotechnology on Nanotechweb.org. in the year 2010.

Cheng-Hsien Liu received his master degree in electrical engineering from Stanford University in 1995 and Ph.D. degree in mechanical engineering from Stanford University in 2000, respectively. Presently he is a professor in the Power Mechanical Engineering Department at National Tsing Hua University. He has been the member of ASME, IEEE, ACS, SPIE, and OSC. His research activities cover a variety of areas in Lab on Chip, Micro Electro Mechanical Systems, System Dynamics/Modeling/Control, microfluidics and Nanotechnology. He received A. Kobayashi Young Investigator Award in Experimental Science from ICCES in 2010, the award of Outstanding Chemical Engineering Article of the Year 2010, the Academic Excellent Award from National Tsing Hua University (2006–2012), Outstanding Research Program Award from National Science and Technology Program in the Biomedical field (2012)and 2011 Outstanding Research Award from National Science Council (NSC), Taiwan in 2012.